Int J Thermophys (2007) 28:947–957
DOI 10.1007/s10765-007-0236-5

Temperature-Dependent Thermal Boundary Conductance at Al/Al_2O_3 and Pt/Al_2O_3 interfaces

Patrick E. Hopkins · R. N. Salaway · R. J. Stevens · P. M. Norris

Published online: 15 August 2007

Abstract With the ever-decreasing size of microelectronic devices, growing applications of superlattices, and development of nanotechnology, thermal resistances of interfaces are becoming increasingly central to thermal management. Although there has been much success in understanding thermal boundary conductance at low temperatures, the current models applied at temperatures more common in device operation are not adequate due to our current limited understanding of phonon transport channels. In this study, the scattering processes in Al and Pt films on Al_2O_3 substrates are examined by transient thermoreflectance testing at high temperatures. At high temperatures, traditional models predict the thermal boundary conductance to be relatively constant in these systems due to assumptions about phonon elastic scattering. Experiments, however, show an increase in the conductance indicating potential inelastic phonon processes.

Keywords Diffuse mismatch model · Elastic scattering · Inelastic scattering · Phonon · Phonon radiation limit · Thermal boundary conductance

1 Introduction

As electronic products become faster and incorporate greater functionality, they are shrinking in size and mass. The continued trend of miniaturization in micro- and opto-

P. E. Hopkins · R. N. Salaway · P. M. Norris (✉)
Department of Mechanical and Aerospace Engineering, University of Virginia, 122 Engineer's Way, Charlottesville, VA 22904-4746, USA
e-mail: pamela@virginia.edu

R. J. Stevens
Department of Mechanical Engineering, Rochester Institute of Technology, Rochester, NY 14623, USA

electronic systems has made the issue of thermal management critical in device design and production. As the length scales continue to decrease, heat transport around active regions in these devices is enhanced/restricted by interfaces between materials and the structures surrounding them. Therefore, accurate predictions of the thermal processes in these devices become dependent on the transport of heat from the device into the packaging material: the thermal boundary conductance across the device/packaging interface [1]. This thermal boundary conductance (h_{BD}) is a controlling factor for thermal management in thermoelectrics [2,3], thin-film high-temperature superconductors [4,5], vertical cavity surface emitting lasers [6], and optical data storage media [7].

An understanding of the basic transport mechanisms involved in thermal boundary conductance is critical to the design and engineering of these devices. The main channel for interfacial thermal transport in the majority of these devices is phonon scattering between two materials. The thermal boundary conductance from phonon scattering can be modeled with the diffuse mismatch model (DMM) or the phonon radiation limit (PRL) [8,9]. The DMM uses information about the distribution of the phonon density of states to calculate the incident phonon flux on the interface; the transmission of the phonon flux is calculated from a combination of the acoustic phonon velocities on either side of the interface. To apply the DMM, the assumption of phonon elastic scattering must be made—i.e., a phonon from side 1 with frequency ω can only scatter with a phonon from side 2 with the same frequency ω. Due to this, h_{BD} is predicted to be constant at temperatures near and above the lower Debye temperature of the two materials comprising the interface since the Debye temperature, θ_{D}, is proportional to the phonon cutoff frequency. Similar assumptions are made in the PRL. The PRL calculates the upper limit of h_{BD} assuming a transmission probability of unity for all phonons that are elastically scattered. These models have been demonstrated to provide good estimates for h_{BD} at low temperatures ($T < 50\,\mathrm{K}$), but at temperatures closer to device operation temperatures, these models do not accurately predict the interfacial thermal processes [10].

In 1993, stoner and Maris reported h_{BD} values for a range of acoustically mismatched interfaces over a temperature range from 50 to 300 K [11,12]. As expected from DMM theory, the measured h_{BD} decreased with sample mismatch, and in each sample, h_{BD} decreased with temperature. In the sample with the greatest mismatch, Pb/diamond, a value of h_{BD} was measured that exceeded the DMM prediction by two orders of magnitude. The measured h_{BD} remained fairly constant, however, over the temperature range, which does not agree with the T^3 trend predicted by the DMM at low temperatures. This measurement also significantly exceeded the prediction of the PRL. One possible explanation offered for this relatively large h_{BD} was the occurrence of inelastic scattering—i.e., one or more phonons of frequency ω_1 were scattering with one or more phonons of frequency ω_2—thereby offering more channels for transport than the DMM accounts for, leading to an underestimate of h_{BD} by the DMM. In this particular case, high-frequency diamond phonons could break down into several low-frequency phonons and scatter with the low-frequency phonons in Pb.

Recently, Chen et al. [13] used molecular dynamics simulations to show a linear increase in h_{BD} across a Kr/Ar nanowire with an increase in temperature from 35 to 55 K. They ascribed this temperature dependence to anharmonic processes. Stevens

Table 1 Thermophysical material properties

Material	Pt	Al	Al_2O_3
υ_L ($m \cdot s^{-1}$)	4174	6240	10890
υ_T ($m \cdot s^{-1}$)	1750	3040	6040
n (m^{-3})	1.1×10^5	1.0×10^5	3.9×10^4
θ_D (K)	240	428	1035
C_l ($T = 300$ K) ($J \cdot m^{-3} \cdot K^{-1}$)	2.83×10^6	2.34×10^6	3.0×10^6
k ($T = 300$ K) ($W \cdot m^{-1} \cdot K^{-1}$)			46
C_l ($T = 400$ K) ($J \cdot m^{-3} \cdot K^{-1}$)	2.89×10^6	2.5×10^6	3.64×10^6
k ($T = 400$ K) ($W \cdot m^{-1} \cdot K^{-1}$)			32.4
C_l ($T = 500$ K) ($J \cdot m^{-3} \cdot K^{-1}$)	2.95×10^6	2.67×10^6	4.04×10^6
k ($T = 500$ K) ($W \cdot m^{-1} \cdot K^{-1}$)			25.6

From top to bottom, the longitudinal phonon velocity [8] the transverse phonon velocity [8] the atomic number density [25], and the Debye temperature [18,26] are important parameters used in DMM and PRL analysis. The lattice specific heat [25] and thermal conductivity [25] are used in fitting the thermal model [10] to the experimental data to determine h_{BD}

et al. [14] observed thermal transport across the interface of two fcc lattice systems with varying degrees of mass and lattice mismatch using molecular dynamics simulations. A linear increase in h_{BD} was observed at temperatures far above the Debye temperatures of the two materials ($T \gg \theta_D$), and the conclusion of inelastic scattering among the phonons in these systems was verified with a detailed wave packet analysis [15]. This linear increase in h_{BD} at $T \gg \theta_D$ was also recently shown experimentally by Lyeo and Cahill [16]. They observed h_{BD} over a temperature range of 80–300 K on carefully prepared Pb and Bi thin films on diamond substrates with a pump-probe thermoreflectance technique. Like Stoner and Maris, Lyeo and Cahill observed h_{BD} magnitudes higher than the PRL but with a linear increase with temperature, thus agreeing with the aforementioned simulation results.

The purpose of this experimental study is to examine the effects that temperatures around and above θ_D have on h_{BD}. This research examines the assumption of phonon elastic scattering by measuring h_{BD} at interfaces with increased temperature ($T > T_{room}$). The trends in h_{BD} predicted by both the DMM and PRL are compared to experimental data from Al and Pt films on Al_2O_3 substrates over a temperature range of 300–500 K using the transient thermoreflectance (TTR) technique. By increasing the temperature around and above the Debye temperatures of the metals in these samples, the entire phonon populations of the films are excited. Assuming elastic scattering, a continued increase in temperature should not significantly affect h_{BD} because all of the phonons in the films are already scattering with the lower-frequency phonons in the substrate. However, results indicate a continued increase in h_{BD} above the film θ_D indicating that higher-frequency substrate phonons activated at the increased temperatures could be scattering with the lower-frequency phonons in the film.

2 Models for Thermal Boundary Conductance

The DMM provides a quick and simple calculation of h_{BD} for an interface between two materials. To apply the DMM in its simplest form, the following assumptions must

be made [17]: (a) phonons are elastically scattered—i.e., a phonon from side 1 with frequency ω can only scatter with a phonon from side 2 with the same frequency ω; (b) phonon scattering is completely diffuse—i.e., a scattered phonon has no memory of the mode (longitudinal or transverse) or direction of the incident phonon; and (c) the materials on both sides of the interface are elastically isotropic—i.e., the longitudinal and transverse acoustic velocities are constant in all crystallographic directions. Assuming a small temperature drop across the interface, the principle of detailed balance can be invoked to calculate h_{BD} [8], the thermal boundary conductance per unit area is given as:

$$h_{\mathrm{BD,\,DMM}} = \frac{1}{4}\sum_j v_{1,j} \int_0^{\omega_{1,j}^{\mathrm{cutoff}}} \alpha_1(\omega)\hbar\omega D_{1,j}(\omega)\frac{\partial f(\omega, T)}{\partial T}\,\mathrm{d}\omega \tag{1}$$

where $v_{1,j}$ is the phonon velocity in side 1 of acoustic phonon mode j (1 longitudinal and 2 transverse), $\alpha_1(\omega)$ is the transmission probability from side 1 to side 2, ω is the angular frequency, $D_{1,j}(\omega)$ is the density of states per unit volume, $\hbar$ is Planck's constant divided by 2π, and $f(\omega, T)$ is the Bose–Einstein distribution function. The cutoff frequency of each phonon mode j on side 1, $\omega_{1,j}^{\mathrm{cutoff}}$, can be calculated for the separate phonon modes from $\omega_{1,j}^{\mathrm{cutoff}} = v_{1,j}(6\pi^2 n_1)^{1/3}$ where n_1 is the atomic density on side 1. The DMM theory assumes that upon scattering, a phonon forgets where it came from, that is, the probability of reflection from one side equals the probability of transmission from the other—i.e., $\alpha_1(\omega) = 1 - \alpha_2(\omega)$. Therefore, according to the principle of detailed balance, the rate at which phonons at a given ω are leaving side 1 into side 2 across the area of the interface must equal the rate at which phonons at the same ω leave side 2 into side 1 across the same area. Assuming a Debye approximation for the phonon density of states per unit volume [18] and applying the principle of detailed balance, the transmission probability is given as:

$$\alpha_1(\omega) = \frac{\sum_j v_{2,j}\frac{\omega^2}{2\pi^2 v_{2,j}^3}}{\sum_j v_{2,j}\frac{\omega^2}{2\pi^2 v_{2,j}^3} + \sum_j v_{1,j}\frac{\omega^2}{2\pi^2 v_{1,j}^3}} = \frac{\sum_j v_{2,j}^{-2}}{\sum_j v_{2,j}^{-2} + \sum_j v_{1,j}^{-2}} = \alpha_1 \tag{2}$$

It is apparent in Eq. 2 that the transmission probability is independent of frequency, which has been verified by molecular dynamics simulations [19]. In fact, the transmission probability is only dependent on the acoustic velocities of the materials on either side of the interface. Substituting Eq. 2 into Eq. 1, h_{BD} as a function of temperature can be calculated. The results of these calculations for Al/Al_2O_3 and Pt/Al_2O_3 systems are shown in Fig. 1. The parameters used in these calculations are summarized in Table 1. Notice that the DMM predicts a constant value of h_{BD} with temperatures above θ_{D} in each material.

As previously discussed, the PRL provides a quick and simple determination of the maximum conductance for interfacial transport from elastic scattering [9]. In cal-

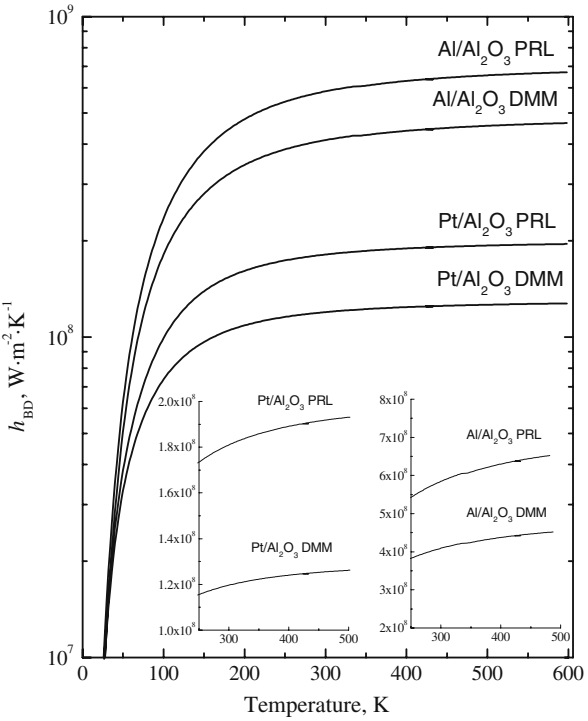

Fig. 1 Thermal boundary conductance calculations of the Al/Al_2O_3 and Pt/Al_2O_3 interfaces using DMM and PRL. Models flatten out at higher temperatures due to the assumption of elastic scattering used in the calculations. Inset graphs show the DMM and PRL for the material systems over only the temperatures used in this work

culations of the PRL, it is assumed that all of the phonons in side 2 up to the cutoff frequency in side 1 (assuming $\omega_{1,j}^{\text{cutoff}} < \omega_{2,j}^{\text{cutoff}}$) contribute to thermal transport though elastic collisions—i.e., $\alpha_2 = 1$. Plugging this and the Debye density of states of side 2 into Eq. 1, the PRL can be rewritten as:

$$h_{\text{BD, PRL}} = \frac{1}{8\pi^2} \sum_j \frac{1}{v_{2,j}^2} \int_0^{\omega_{1,j}^{\text{cutoff}}} \hbar\omega^3 \frac{\partial f(\omega, T)}{\partial T} \, \mathrm{d}\omega \tag{3}$$

The results of the PRL for Al/Al_2O_3 and Pt/Al_2O_3 are shown in Fig. 1 with parameters listed in Table 1. Since the PRL represents the upper limit of the elastic contribution to thermal transport, it will always predict a higher h_{BD} than the DMM. Notice that, like the DMM, the PRL predicts a constant h_{BD} at high temperatures ($T \sim \theta_D$). The insets of Fig. 1 show a close-up of the DMM and PRL calculations for the two materials systems in the temperature range of interest in this study.

3 Experimental Considerations

3.1 Samples

Since the goal of this study is to examine any deviations of h_{BD} from the DMM and PRL elastic scattering assumptions at high temperatures, material systems were chosen to encompass different regimes in which the amount of temperature dependence in h_{BD}, as predicted by DMM, would vary. The Pt/Al_2O_3 and Al/Al_2O_3 material systems allow investigation of h_{BD} at temperatures around θ_D of Al and well above θ_D of Pt. Assuming elastic scattering, an increase in h_{BD} is expected in Al over the temperature range since the phonon population will increase until $T > \theta_D$. However, in Pt where $\theta_D < T_{room}$ an increase in h_{BD} should not occur since the entire phonon population is excited. Any increase when $T > \theta_D$ could be evidence of a high-frequency substrate phonon exciting from the elevated temperature and scattering with two or more lower-frequency film phonons.

The Al and Pt film thicknesses were 75 and 50 nm, respectively, chosen to be ~50% greater than the electron mean free path in these metals to minimize electron scattering at the boundary since the interest in this study is interfacial phonon transport [20]. These thicknesses were also necessary to ensure that it was possible to extract viable h_{BD} information from the TTR data [10]. The Al and Pt films were deposited on factory polished Al_2O_3. The depositions took place in a multisource, high vacuum thin film sputter deposition system, a Supersystem III manufactured by the Kurt J. Lesker Company capable of pumping down to 10^{-7} Torr. All substrates were (ETM) spin cleaned with reagent alcohol (90.7% ethyl alcohol; 4.8% isopropyl alcohol; 4.5% methyl alcohol; 0.12% water), trichloroethylene, and methanol, then subsequently baked for 5 min at 400 K to remove any residual water that may have formed at the substrate surface as a result of the spin clean. The substrates were subjected to a 5 min, 100 W backsputter etch prior to film deposition to remove the oxide layer and any additional contaminants.

3.2 Experimental Setup

The TTR data were taken with a pump-probe experimental setup where the primary output of the laser system emanates from a Coherent RegA 9000 amplifier operating at a 250 kHz repetition rate with about 4 μJ per pulse and a 150 fs pulse width at 800 nm. The pulses were split at a 9:1 pump to probe ratio. The pump beam, modulated at 125 kHz, was focused down to a 100 μm radius spot size to achieve 10 J·m^{-2} fluence. The probe beam was focused to the middle of the pump beam to achieve a pump-to-probe fluence ratio of 10:1. The radii of the pump and probe beams were measured with a sweeping knife edge [21]. Although the low repetition rate of the RegA system and the "one shot on—one shot off" modulation rate of the pump beam ensures minimal residual heating between pump pulses, the phase of the signal must still be taken into account. The phase correction was performed by the procedures for signal phase adjustment outlined in the references [21].

For long scans, alignment of the pump and probe spots can become an issue [10,21, 22]. To avoid misalignment problems, the probe beam was collimated before the probe delay stage and profiled with a sweeping knife-edge at all time delays. In this study, a pump to probe radius ratio of 10:1 was used, and the probe was aligned with the delay stage resulting in less than 1.5 and 4.0 μm drift along the horizontal and vertical axes perpendicular to the surface, respectively. These spot characteristics result in less than 1% error due to misalignment of the beams [21].

The samples were mounted to a 5 mm thick Al plate attached to a Minco 5419 silicon rubber resistive heater. The samples were mounted on the front of the Al plate with Molykote 44 high-temperature vacuum grease, and the sides and back of the aluminum plate/heater were insulated with high-temperature millboard insulation. Thermocouple holes were drilled 1 mm underneath the front surface of the Al plate in four locations surrounding the sample to monitor the temperature of the sample. For each desired temperature, the Al block was heated and held at constant temperature for ~2 h to ensure that the sample/Al block system equilibrated before TTR measurements were taken. After several measurements at a certain temperature, the heater was turned off and the temperature dropped to room temperature. Room-temperature measurements were again taken after the system returned to room conditions, and these measurements were compared to ensure that the sample was not damaged as a result of the heating, The value of h_{BD} was determined by fitting the TTR data to the thermal model discussed in detail in Stevens et al. [10]. Repeatable results were found at all temperatures. The data presented in this article are the statistical averages of the data at each temperature, and a deviation of less than 10% from the mean was calculated.

4 Results

The TTR data are plotted against temperature for the Al and Pt material systems in Figs. 2 and 3, along with the calculations for the DMM and PRL in these systems. The line fit to the data depicts the linearity of the relationship between temperature and h_{BD} observed in the experiments. The slope of this line, η, is also presented in these figures along with the Debye temperatures of the materials. Figure 2 shows the measured h_{BD} across the Al/Al_2O_3 interface. In addition to data measured in this study ($300\,K < T < 500\,K$), low-temperature data from Stoner and Maris [12] are included. The linear fit included the data from this study and Stoner and Maris data from 150 K to room temperature. At 150 K, h_{BD} appears to loose its T^3 dependence. Over the temperature range in this study, the experimental data increases by almost 100%, where the DMM, which would consider only elastic scattering, only predicts a 10% increase. In addition, the data above θ_D of Al increase 25% over a 50 K temperature increase. The linear increase above θ_D of Al suggests that inelastic phonon processes may occur between a single high-frequency phonon in the Al_2O_3 and two or more lower-frequency phonons in Al. As the temperature is driven above θ_D of Al, the entire phonon population in Al is excited. However, the linear increase of Al_2O_3 phonon population continues and, therefore, the increase in h_{BD} above the θ_D of Al could be evidence of inelastic scattering. The continued linear trend observed from the data from Stoner and Maris to the high-temperature data even above θ_D of Al,

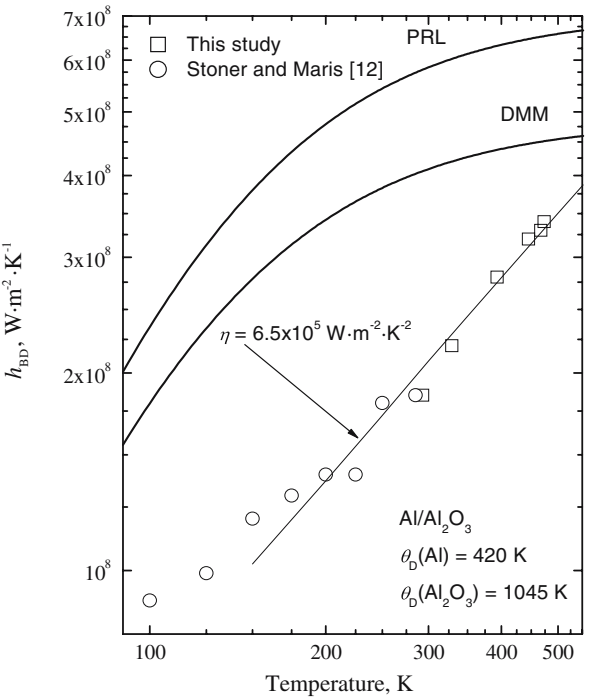

Fig. 2 Measured thermal boundary conductance across the Al/Al_2O_3 boundary from this work (squares) and from Stoner and Maris (circles) [12]. Increase in h_{BD} with temperature is much greater than that predicted from the DMM and PRL, which could be evidence of inelastic phonon collisions contributing to h_{BD}. Inelastic scattering is not taken into account in the theoretical models

indicates that there is a smooth transition between regimes where h_{BD} is dominated by elastic and inelastic scattering.

To examine the regime where inelastic scattering would dominate (i.e., temperatures above the Debye temperature of only one of the materials, so that the entire phonon population of one material is excited but not the other), the highly mismatched Pt/Al_2O_3 system was studied. Lyeo and Cahill [16] found this regime at low temperatures with Pb and Bi on diamond. The Al/Al_2O_3 system gives hints towards anharmonic processes with the data 50 K above θ_D. However, due to the less than room temperature θ_D of Pt, the highly mismatched Pt/Al_2O_3 shows promising data that further support the findings of inelastic scattering processes in high-temperature regimes. Figure 3 shows h_{BD} versus temperature TTR results. The temperature of this interface was increased to over twice θ_D of Pt. Over the investigated temperature range, h_{BD} increases by over 50%, which is a similar result to previous calculations that model elastic and inelastic scattering [14]. The DMM and PRL predict an increase in h_{BD} of less than 5% over this temperature range. Since the change in the Pt phonon population is constant above $\theta_{D,Pt}$, the linear increase in h_{BD} observed in the TTR data indicates that inelastic phonon processes are occurring.

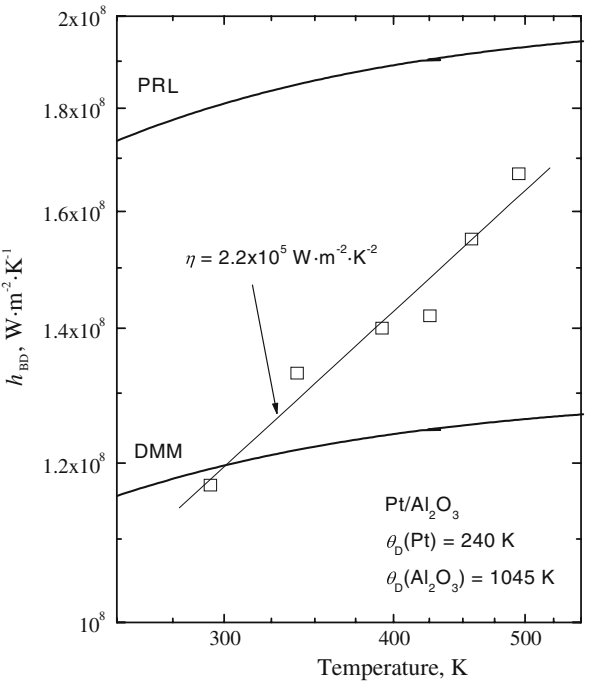

Fig. 3 Measured thermal boundary conductance across the Pt/Al_2O_3 boundary. Change in h_{BD} at these high temperatures ($T \gg \theta_{D,Pt}$) is linear where the change in h_{BD} predicted from the DMM and PRL assuming only elastic collisions contributing to transport is relatively flat

The experimental data in this study are compared to the DMM and PRL models which were calculated assuming a Debye density of states. The Debye density of states provides a quick and simple calculation of the DMM and PRL; however, several studies have showed that using a more realistic density of states could significantly change the resulting calculations [19,23,24]. Recent calculations by Reddy et al. [23] of metal films on semiconductor substrates use the Born von-Karmen approximation (BKM) to calculate an exact phonon dispersion in the DMM. The trend in the models resulting from these calculations (i.e., change in h_{BD} with temperature which becomes negligible at temperatures approaching θ_D) changes with the BKM calculation [23]. With this more realistic density of states, the change in h_{BD} with temperature becomes negligible at much lower temperatures. Applying this conceptual shift to the DMM and PRL data results in an even more drastic difference between the trends in the experimental data and the trends in the models assuming only elastic phonon collisions presented in Figs. 2 and 3. This gives further evidence that inelastic scattering events are participating in h_{BD} at higher temperatures.

Comparing the slopes of h_{BD} versus temperature of the Al/Al_2O_3 and Pt/Al_2O_3 samples gives interesting insight into the contributions of the elastic and inelastic processes. The slope of the data on Pt/Al_2O_3, which is taken at temperatures well above $\theta_{D,Pt}$, is $\eta = 2.2 \times 10^5\,W \cdot m^{-2} \cdot K^{-2}$ calculated from the best fit line estimate to the data. However, for the Al/Al_2O_3 sample, $\eta = 6.5 \times 10^5\,W \cdot m^{-2} \cdot K^{-2}$, nearly three

times greater than that of the Pt/Al_2O_3 sample. Over the temperature range of the data for Al/Al_2O_3 presented in Fig. 2, the increase in h_{BD} can be attributed to both elastic and inelastic scattering. In the event of inelastic scattering, a high-frequency Al_2O_3 phonon does not need to break down into many low-frequency phonons for energy transmission. However, over the temperature range of the data for Pt/Al_2O_3 presented in Fig. 3, for reasons previously discussed, the continued increase can be ascribed to inelastic scattering. Due to the low Debye temperature of Pt, an Al_2O_3 phonon would have to break down several times for energy transmission (more times than for energy transmission from Al). This large phonon decomposition cascade could reduce energy transmission, therefore partly causing η for the Pt/Al_2O_3 sample to be less than η for the Al/Al_2O_3 sample. Contributions of elastic scattering in the measured h_{BD} on the Al/Al_2O_3 sample could also add to this difference in η.

5 Conclusions

Thermal management in micro- and opto-electronic devices is becoming critical to further development. The mechanisms of interfacial phonon transport must be fully understood to accurately predict thermal processes in these devices. Although traditional models predict thermal boundary conductance at low temperatures ($T \ll T_{room}$) relatively well, at temperatures closer to device operating temperatures these models fail to account for inelastic phonon scattering processes which could contribute to interface conductance. To test the effect of these inelastic processes, TTR experiments were performed on Al and Pt films on Al_2O_3 substrates at elevated temperature ($T > T_{room}$). At these temperatures, the thermal boundary conductance is assumed to be relatively constant by traditional models considering only elastic scattering. At temperatures around and above the Debye temperature of the metal film, the thermal boundary conductance was shown to increase linearly with temperature indicating that inelastic scattering is contributing to interfacial transport.

Acknowledgments This work was funded by the National Science Foundation (CTS—0536744). Patrick Hopkins is greatly appreciative for financial support from the National Science Foundation through the Graduate Research Fellowship Program. The authors would also like to thank Mike Klopf, Jenni Simmons, and Jes Sheehan for insightful discussions.

References

1. D.G. Cahill, W.K. Ford, K.E. Goodson, G.D. Mahan, A. Majumdar, H.J. Maris, R. Merlin, S.R. Phillpot, J. Appl. Phys. **93**, 793 (2003)
2. L.W. da Silva, M. Kaviany, Int. J. Heat Mass Transfer **47**, 2417 (2004)
3. G.D. Mahan, L.M. Woods, Phys. Rev. Lett. **80**, 4016 (1998)
4. P.E. Phelan, Y. Song, O. Nakabeppu, K. Ito, K. Hijikata, T. Ohmori, K. Torikoshi, J. Heat Transfer **116**, 1038 (1994)
5. P.E. Phelan, J. Heat Transfer **120**, 37 (1998)
6. G. Chen, C.L. Tien, X. Wu, J.S. Smith, J. Heat Transfer **116**, 325 (1994)
7. E.-K. Kim, S.-I. Kwun, S.-M. Lee, H. Seo, J.-G. Yoon, Appl. Phys. Lett. **76**, 3864 (2000)
8. E.T. Swartz, R.O. Pohl, Rev. Mod. Phys. **61**, 605 (1989)
9. N.S. Snyder, Cryogenics **10**, 89 (1970)
10. R.J. Stevens, A.N. Smith, P.M. Norris, J. Heat Transfer **127**, 315 (2005)

11. The term "acoustic mismatch" describes two materials that have significantly different acoustic velocities; the degree of the acoustic mismatch can be easily determined by comparing the materials' Debye temperatures, θ_D
12. R.J. Stoner, H.J. Maris, Phys. Rev. B **48**, 16373 (1993)
13. Y. Chen, D. Li, J. Yang, Y. Wu, J. Lukes, A. Majumdar, Physica B **349**, 270 (2004)
14. R.J. Stevens, L.V. Zhigilei, P.M. Norris, Int. J. Heat Mass Transfer (in press)
15. P.K. Schelling, S.R. Phillpot, P. Keblinski, Phys. Rev. B **65**, 114306 (2002)
16. H.-K. Lyeo, D.G. Cahill, Phys. Rev. B **73**, 144301 (2006)
17. D.G. Cahill, A. Bullen, S.-M. Lee, High Temp.-High Press **32**, 135 (2000)
18. C. Kittel, *Introduction to Solid State Physics* 7th edn. (John Wiley and Sons, Inc., New York, 1996).
19. D.A. Young, H.J. Maris, Phys. Rev. B **40**, 3685 (1989)
20. J. Hohlfeld, S.-S. Wellershoff, J. Gudde, U. Conrad, V. Jahnke, E. Matthias, Chem. Phys. **251**, 237 (2000)
21. R.J. Stevens, A.N. Smith, P.M. Norris, Rev. Sci. Instrum. **77**, 084901 (2006)
22. W.S. Capinski, H.J. Maris, Rev. Sci. Instrum. **67**, 2720 (1996)
23. P. Reddy, K. Castelino, A. Majumdar, Appl. Phys. Lett. **87**, 211908 (2005)
24. B.C. Daly, H.J. Maris, K. Imamura, S. Tamura, Phys. Rev. B **66**, 024301 (2002)
25. D.E. Gray, *American Institute of Physics Handbook* 3rd edn. (McGraw Hill, New York, 1972)
26. R.Q. Fugate, C.A. Swenson, J. Appl. Phys. **40**, 3034 (1969)